*Korean J. Chem. Eng.*, **21**(4), 836-852 (2004)

# An Optimization Strategy for Nonlinear Simulated Moving Bed Chromatography: Multi-Level Optimization Procedure (MLOP)

**Young-Il Lim**†

Department of Chemical Engineering, Hankyong National University,
67 Sukjung-dong, Anseong-si, Kyonggi-do 456-749, Korea
(*Received 31 October 2003 • accepted 16 February 2004*)

**Abstract**–This paper presents a multi-level optimization strategy to obtain optimum operating conditions (four flowrates and cycle time) of nonlinear simulated moving bed chromatography. The multi-level optimization procedure (MLOP) approaches systematically from initialization to optimization with two objective functions (productivity and desorbent consumption), employing the standing wave analysis, the true moving bed (TMB) model and the simulated moving bed (SMB) model. The procedure is constructed on a non-worse solution property advancing level by level and its solution does not mean a global optimum. That is, the lower desorbent consumption under the higher productivity is successively obtained on the basis of the SMB model, as the two SMB-model optimizations are repeated by using a standard SQP (successive quadratic programming) algorithm. This approach takes advantage of the TMB model as well as surmounts shortcomings of the TMB model in the general case of any nonlinear adsorption isotherm using the SMB model. The MLOP is evaluated on two nonlinear SMB cases characterized by i) quasi-linear/non-equilibrium and ii) nonlinear/nonequilibrium model. For the two cases, the MLOP yields a satisfactory solution for high productivity and low desorbent consumption within required purities.

Key words: Simulated Moving Bed (SMB) Chromatography, Simulation and Optimization, Multi-Level Optimization Procedure (MLOP), Nonlinear Adsorption Isotherms, Productivity, Desorbent Consumption

## INTRODUCTION

Simulated Moving Bed (SMB) processes have emerged as a promising technology for the separation of not only conventional compounds, e.g., petro-chemicals [Kim et al., 2001] and sugar [Beste et al., 2000; Lee, 2003], but also pharmaceuticals, e.g., chiral compounds [Pais et al., 1998], and bio-chemicals, e.g., amino acids, peptides and proteins [Juza et al., 2000]. SMB chromatography usually works with the inherent advantage of a high driving force, resulting in less solvent consumption, smaller apparatus scale, lower investment costs and higher yields. However, in order to fully take advantage of this principle, a large number of operational parameters (e.g., flowrates, switching time, column dimension and configuration) need to be adjusted properly [Klatt et al., 2002]. Since an experimental evaluation of these operational parameters is very time consuming and costly [Kim et al., 2001], model-based simulation and optimization can help to effectively search optimum operation conditions.

In SMB applications, throughput (or productivity) and desorbent consumption are two key factors that control process cost [Wu et al., 1999]. Practically, the operating conditions are selected to reach the maximum productivity with the lowest elution consumption [Mazzotti et al., 1997; Ludemann-Hombourger et al., 2002].

A four-zone linear SMB process for paclitaxel purification is optimized on the two key factors subject to purity and pressure drop in terms of four flowrates and column configuration [Wu et al., 1999]. An optimization algorithm for the design of SMB processes is presented by Biressi et al. [2000], using a steady-state TMB model with the equilibrium adsorption assumption for productivity and purity evaluation. The column length is chosen at a maximum productivity defined as feeding mass of solute per unit time and volume of solid phase. A bi-objective optimization approach considering both productivity and extract purity objectives is proposed for a chiral SMB chromatography, where constraints are raffinate purity, pressure drop and the optimization variables are flow rates, switching time and column configuration [Zhang et al., 2002 and 2003].

Proll and Kusters [1998] proposed a two-step approach including the optimization step and the adaptation step for adsorption isotherm model modification. In the optimization step, a productivity function is maximized in terms of four flowrates, feed concentrations and switching time, where the equilibrium adsorption model with a true moving bed (TMB) assumption at the steady-state is used for productivity evaluation. The first step is repeated once after the adsorption model verification step by experiments.

A multi-step optimization procedure is proposed in a heuristic manner, separating the TMB model simulation from the SMB model simulation [Beste et al., 2000]. The feed flowrate and feed concentrations are fixed because of operation and solubility problems. The optimization variable is desorbent, extract and raffinate flowrates, and the switching time. By steady-state TMB model simulation, the three flowrates are decided with desired purity, yield and productivity and then the switching time with desired dilution. The two steps are repeated until required conditions are obtained. At the final step, the TMB optimization results are checked with the SMB model simulation because the SMB model is much closer to reality.

Klatt et al. [2002] proposed a model-based optimization proce-

†To whom correspondence should be addressed.
E-mail: limyi@hnu.hankyong.ac.kr

**Table 1. Comparison of this study with other optimization procedures for SMB processes**

| Authors | Models | Objective functions | Variables | Constraints | Given data | Remarks |
|---|---|---|---|---|---|---|
| Proll and Kusters (1998) | -nonlinear isotherm -equilibrium stage -steady-state TMB | productivity | $Q_{feed}$, $Q_{ext}$, $Q_{rec}$, $Q_{des}$, $\tau$ | purity, $\Delta p$ | $L_c$, $\varepsilon_b$, $K_i$ | Model adaptation algorithm is included. |
| Wu et al. (1999) | -linear isotherm -(non)equilibrium -steady-state TMB | throughput $Q_{des}/Q_{feed}$ | column design parameters, $Q_{feed}$, $Q_{des}$ | purity, $\Delta p$ | $\varepsilon_b$, $K_i$, k, $D_{ax}$, $C_{feed}$, $\tau$ | Analytically-obtained objective functions |
| Biressi et al. (2000) | -nonlinear isotherm -equilibrium stage -steady-state TMB | productivity | $L_c$, $Q_{feed}$, $Q_{ext}$, $Q_{rec}$, $Q_{des}$, $\tau$ | purity, $\Delta p$ | $\varepsilon_b$, $\varepsilon_p$, $K_i$, $n^*$, $C_{feed}$ | Optimization of design and operating variables |
| Beste et al. (2000) | -nonlinear isotherm -nonequilibrium -steady-state TMB | heuristic iteration | $Q_{ext}$, $Q_{rec}$, $Q_{des}$, $\tau$ | purity, yield, productivity | $L_c$, $\varepsilon_b$, $n^*$, $Q_{feed}$, $C_{feed}$, k, $D_{ax}$ | SMB model verification |
| Klatt et al. (2002) | -(non)linear isotherm -nonequilibrium -SMB | $Q_{des}$ | $Q_{ext}$, $Q_{rec}$, $Q_{des}$, $\tau$ (see remarks) | purity, $\Delta p$ | $L_c$, $\varepsilon_b$, $n^*$, $Q_{feed}$, $C_{feed}$ | Safety factors are used as variables instead of flowrates |
| Zhang et al. (2003) | -nonlinear isotherm -equilibrium stage -SMB | purity, productivity | $Q_{feed}$, $Q_{ext}$, $Q_{rec}$, $Q_{des}$, $\tau$ | purity, $\Delta p$ | $L_c$, $\varepsilon_b$, $n^*$, $C_{feed}$ | Multiobjective optimization using a genetic algorithm |
| This study | -nonlinear adsorption -nonequilibrium -TMB/SMB | productivity, $Q_{des}$ | $Q_{feed}$, $Q_{ext}$, $Q_{rec}$, $Q_{des}$, $\tau$ | purity, $\Delta p$ | $L_c$, $\varepsilon_b$, $n^*$, $K_i$, k, $D_{ax}$, $C_{feed}$ | Multilevel optimization using SQP algorithm |

dure in the case that the plant design is fixed, and the feed flowrate and concentration are prespecified. Here, the desorbent flowrate constitutes the only variable contribution to the process operating cost. Thus, the desorbent flowrate is minimized in terms of the desorbent, extract, recycle flowrates and the cycle time, constrained by extract and raffinate purities and an allowable flowrate at each section. Since the accuracy of TMB approximation can be poor at nonlinear cases, the SMB model is recommended for more reliable simulation. However, the SMB optimization problem is not well-conditioned from a numerical point of view [Klatt et al., 2002]. Four safety factors for the ratio of the net mass flowrate of the solid and the liquid phase are considered as the optimization variables instead of the three flowrates and the cycle time. The purity constraints are evaluated by the SMB model that can predict cyclic behaviors of the SMB operation.

In Table 1, characteristics of the six-optimization studies mentioned above are compared with those of this study to be described. This study aims to identify SMB operating conditions at a minimum desorbent consumption subject to a satisfactory productivity, using a rigorous SMB model (e.g., nonlinear and nonequilibrium adsorption SMB model) that supplements the TMB model employed in the preliminary optimization steps. Therefore, this approach takes advantage of the TMB model as well as surmounts shortcomings of the TMB model in the general case of nonlinear adsorption isotherms.

To achieve this purpose, a multi-level optimization procedure (MLOP) is proposed for optimization of a four-zone nonlinear SMB chromatography. The MLOP systematically approaches from initialization to optimization and from simple models (e.g., linear isotherms) to complex models (e.g., nonlinear and nonequilibrium adsorption models).

The remainder of the paper is organized as follows. Section 2 describes theoretical backgrounds and explains each level of the MLOP. In section 3, two examples referred to the literature are illustrated to show the evidence of robustness of this procedure. Section 4 concludes this work.

## MULTI-LEVEL OPTIMIZATION PROCEDURE (MLOP)

When the column dimension and configuration are given for a target mixture in the four-zone SMB, operating variables such as desorbent ($Q_{des}$), extract ($Q_{ext}$), feed ($Q_{feed}$), recycle ($Q_{rec}$) flowrates and the cycle time ($\tau$) should properly be adjusted to obtain desirable process performances (e.g., productivity, desorbent consumption, purities and yields). Flowrates at the four zones such as zone I (desorbent-extract), zone II (extract-feed), zone III (feed-raffinate) and zone IV (raffinate-desorbent) are expressed:

$$Q_I = Q_{des} + Q_{rec} \quad (1a)$$

$$Q_{II} = Q_{des} + Q_{rec} - Q_{ext} \quad (1b)$$

$$Q_{III} = Q_{des} + Q_{rec} - Q_{ext} + Q_{feed} \quad (1c)$$

$$Q_{IV} = Q_{rec} \quad (1d)$$

The five operating conditions are selected to reach the maximum productivity with the lowest desorbent consumption [Ludemann-Hombourger et al., 2002]. However, it is highly ideal to achieve these two objectives at the same time. In other words, this optimization problem aims to obtain a utopia point [Lim et al., 1999] in the two-objective space. In this study, we consider a min-max optimization problem such that desorbent consumption ($Q_{des}$) is mini-

mized within a certain range (or relaxation value) of a maximum productivity constrained by desirable extract ($a_1$) and raffinate ($a_2$) purities as well as allowable pressure drop (or flowrate of zone I, $a_3$). The optimization variable set (**X**) contains the 5 operating variables, $X \in \{\tau, Q_{des}, Q_{ext}, Q_{feed}, Q_{rec}\}$. The problem is formulated as follows:

$$\begin{aligned} &\underset{X}{\text{Min}} Q_{des} \\ &\text{s.t. } \text{Pr} \geq \xi(\underset{X}{\text{Max}}\,\text{Pr}) \\ &\quad \text{s.t.} (\text{Pu})_{ext} \geq a_1 \\ &\quad\quad (\text{Pu})_{raf} \geq a_2 \\ &\quad\quad (Q_{rec} + Q_{des}) \leq a_3 \end{aligned} \tag{2}$$

where $\xi$ is the relaxation factor with the range $0<\xi\leq 1$, and the productivity (Pr) and purities ($\text{Pu}_{ext}$ and $\text{Pu}_{raf}$) are defined:

$$\text{Pr} \equiv \text{Pr}_{ext} + \text{Pr}_{raf} = \frac{1}{(1-\varepsilon_b)N_c V_c}(Q_{ext}\overline{C}_{B,ext} + Q_{raf}\overline{C}_{A,raf}) \tag{3a}$$

$$\text{Pr} = \frac{1}{(1-\varepsilon_b)N_c V_c}(Q_{feed}C_{T,feed}) \tag{3b}$$

$$\text{Pu}_{ext} = \frac{\overline{C}_{B,ext}}{\overline{C}_{A,ext} + \overline{C}_{B,ext}} \tag{4a}$$

$$\text{Pu}_{rat} = \frac{\overline{C}_{A,rat}}{\overline{C}_{A,rat} + \overline{C}_{B,rat}} \tag{4b}$$

where $\overline{C}_{A,ext}$, $\overline{C}_{B,ext}$, $\overline{C}_{A,raf}$ and $\overline{C}_{B,raf}$ denote the average concentration of A or B in extract or in raffinate, respectively. In Eq. (3), the number of columns ($N_c$), the column volume ($V_c$) and the bed voidage ($\varepsilon_b$) are the physical characteristics of the column. In Eq. (3b), the total feed concentration is defined as $C_{T,feed}=C_{A,feed}+C_{B,feed}$. Here, A is the less retained (or fast going) component and B is the more retained (or slow going) component. Consequently, the component A is rich in the raffinate and the component B is rich in the extract. Note that the productivity function can be defined in many different forms, and Eq. (3a) or (3b) is usually used in SMB optimization problems [Wu et al., 1999; Beste et al., 2000]. Productivity and purity are evaluated by the nonequilibrium SMB model described as a distributed dynamic model with periodic port switching [Pais et al., 1998; Lim and Jørgensen, 2004]:

$$\frac{\partial C}{\partial t} = -v_L\frac{\partial C}{\partial z} + D_{ax}\frac{\partial^2 C}{\partial z^2} - \phi k(n^* - n) \tag{5a}$$

$$\frac{\partial n}{\partial t} = k(n^* - n) \tag{5b}$$

$$n^* = g(C) \tag{5c}$$

where $v_L$ is the interstitial velocity, $D_{ax}$ is the axial dispersion coefficient and $\phi$ is the phase ratio defined as $\phi=(1-\varepsilon_b)/\varepsilon_b$. The liquid and solid concentrations for each component are referred to as C and n, respectively. $n^*$ is the equilibrium concentration (adsorption isotherm) that is normally defined as a function of liquid concentrations, g(C). A conventional linear driving force (LDF) model with a lumped mass transport coefficient (k) is employed in Eq. (5b) for the adsorption kinetic. When k becomes large, Eq. (5) is close to the equilibrium model ($\partial n/\partial t=\partial n^*/\partial t$). If g(C) in Eq. (5c) is expressed as $g_i(C)=K_iC_i$ for each component, it is called a linear system. If not, the chromatographic system is nonlinear. Notice that $v_L$, $D_{ax}$, and k are zone-dependent variables or parameters. Eq. (5) is solved with initial conditions (IC: $C_0$ and $n_0$) and boundary conditions (BC: $C_{z=0}$ and $C_{z=L_c}$):

$$\text{IC} = \begin{cases} C(z,0) = C_0, \forall z \\ n(z,0) = n_0, \forall z \end{cases} \tag{6}$$

$$\text{BC} = \begin{cases} v_L(C_{z=0} - C_{in}) = D_{ax}\left.\dfrac{\partial C}{\partial z}\right|_{z=0}, \forall t \\ \left.\dfrac{\partial C}{\partial z}\right|_{z=L_c} = 0, \forall t \end{cases} \tag{7}$$

where $C_{in}$ is the inlet concentration entering to each column, which is given as SMB operating conditions:

$$\begin{cases} Q_{in}^i = Q_{out}^{i-1} + \lambda_1 Q_{feed} + \lambda_2 Q_{des} - \lambda_3 Q_{ext} - \lambda_4 Q_{raf} \\ C_{in}^i \cdot Q_{in}^i + C_{out}^{i-1} \cdot Q_{out}^{i-1} + \lambda_1 C_{feed} \cdot Q_{feed} + \lambda_2 C_{des} \cdot Q_{des} \\ \qquad - \lambda_3 C_{out}^{i-1} \cdot Q_{ext} - \lambda_4 C_{out}^{i-1} \cdot Q_{raf} \end{cases} \tag{8}$$

where the superscript i denotes the column number (or zone) and $\lambda_1-\lambda_4$ are logical variables (0 or 1) according to the port switching. In this paper, the nonequilibrium SMB model includes Eq. (5)-(8). In the TMB model, Eq. (5b) is replaced by:

$$\frac{\partial n}{\partial t} = v_S\frac{\partial n}{\partial z} + k(n^* - n) \tag{9}$$

where $v_S$ is the solid velocity ($v_S=L_c/\tau$) in terms of the column length ($L_c$) and the cycle time ($\tau$). Therefore, the nonequilibrium TMB model [Pais et al., 1998] includes Eq. (5a), (9), (5c), and (6)-(7) without the port switching Eq. (8). When the time derivatives in Eq. (5a) and (9) are equal to zero, the steady-state TMB model [Proll and Kusters, 1998; Beste et al., 2000] is obtained.

Note that the equivalence between the TMB and the SMB models is made by keeping constant the liquid velocity relative to the solid velocity [Ma and Wang, 1997; Mazzotti et al., 1997; Pais et al., 1998; Biressi et al., 2000]. That is, the liquid velocity in SMB is:

$$(v_L)_{SMB} = (v_L)_{TMB} + v_S \tag{10}$$

The relationship Eq. (10) is applied only for the recycle flowrate and flowrates of each column are sequentially influenced.

$$(Q_{rec})_{SMB} = (Q_{rec})_{TMB} + \varepsilon_b S v_S \tag{11}$$

For different column dimension and configuration, the optimization problem Eq. (2) is repeated, where the number of columns ($N_c$) and the column volume ($V_c$) are taken into account in Eq. (3). When the column dimension is given, an optimum solution is found by examining desorbent consumption and productivity optimized for each column configuration.

It is worth noting that the desorbent consumption is minimized within a satisfactory productivity rather than a compromise between the two objective functions. Therefore, Eq. (2) will find a specific optimum point of the multiobjective optimization results (or Pareto points, Lim et al., 1999). If the Pareto line is convex within the two-objective space, Eq. (2) has only one global optimum point that $\xi(\underset{X}{\text{Max}}\,\text{Pr})$ with the three constraints in Eq. (2) produces. However, if this sys-

tem is not convex, Eq. (2) can have several local optimum points in the multiobjective space.

Unfortunately, the min-max problem with the SMB model Eq. (5)-(8) is not well-conditioned from a numerical point of view [Klatt et al., 2002], because the SMB model used for productivity and purity evaluation in Eq. (3)-(4) shows cyclic behavior of the concentrations within the switching time (or cycle time), and their average value (e.g., $\overline{C}_{B,ext}$ or $\overline{C}_{A,raf}$) may be same at multiple operating conditions. That is, the optimization problem can be nonconvex and fail to converge when a gradient-based method such as SQP (successive quadratic programming) is employed for Eq. (2). A global optimization method such as the genetic algorithm [Zhang et al., 2002 and 2003] can be useful for this SMB optimization problem. However, substantial computational time is required for the global optimization techniques. This study addresses an optimization strategy to efficiently solve Eq. (2) by using a standard SQP algorithm [Powell, 1971]. In the following section, Eq. (2) is decomposed into two optimization problems coupled, identifying a minimum set of optimization variables.

**1. Decomposition of the Min-max Problem**

Eq. (2) is equivalent to the following decomposed equations:

$$\begin{aligned} &\max_{X} \mathrm{Pr} \\ &\text{s.t.} (\mathrm{Pu})_{ext} \geq a_1 \\ &\quad (\mathrm{Pu})_{raf} \geq a_2 \\ &\quad (Q_{rec}+Q_{des}) \leq a_3 \end{aligned} \tag{12a}$$

$$\begin{aligned} &\min_{X} Q_{des} \\ &\text{s.t.} \mathrm{Pr} \geq \xi \mathrm{Pr}^{max} \\ &\quad (\mathrm{Pu})_{ext} \geq a_1 \\ &\quad (\mathrm{Pu})_{raf} \geq a_2 \\ &\quad (Q_{rec}+Q_{des}) \leq a_3 \end{aligned} \tag{12b}$$

where $\mathrm{Pr}^{max}$ is the resulting value of Eq. (12a) and Eq. (12b) is solved within a relaxed value ($\xi$) of $\mathrm{Pr}^{max}$. Since both of the two optimization problems are also ill-conditioned like Eq. (2), an iterative problem between the two problems is designed, decomposing the variable space (X) into $X_1$ and $X_2$, $X \in \{X_1, X_2\}$. Due to the variable decomposition, the relaxation factor can be removed. In the first stage, the productivity is considered as an objective function in order to fully exploit the given process, adjusting $X_1$. In the next stage, the desorbent consumption is reduced, keeping the productivity maximized and adjusting $X_2$.

$$\begin{aligned} &\max_{X_1} \mathrm{Pr} \\ &\text{s.t.} (\mathrm{Pu})_{ext} \geq a_1 \\ &\quad (\mathrm{Pu})_{raf} \geq a_2 \\ &\quad (Q_{rec}+Q_{des}) \leq a_3 \end{aligned} \tag{13a}$$

$$\begin{aligned} &\min_{X_2} Q_{des} \\ &\text{s.t.} \mathrm{Pr} \geq \xi \mathrm{Pr}_{X_1}^{max} \\ &\quad (\mathrm{Pu})_{ext} \geq a_1 \\ &\quad (\mathrm{Pu})_{raf} \geq a_2 \\ &\quad (Q_{rec}+Q_{des}) \leq a_3 \end{aligned} \tag{13b}$$

Here, $X_1$ should be defined as a minimum set of optimization variables with which the objective function and the constraints independently change. Once $X_1$ is obtained, let $X_2$ be $(X-X_1)$. If Eq. (13a) and (13b) are successfully repeated by using the two variable spaces decomposed, it is guaranteed that the final solution obtained after a stop-criterion yields a minimum desorbent flowrate at the higher productivity. If not, Eq. (13) remains ill-conditioned like the original problem Eq. (2). Thus, a global optimization technique might be needed.

To have an idea for the variable space decomposition, the standing wave analysis proposed by Ma and Wang [1997] for binary systems with linear isotherms and nonequilibrium adsorption is introduced, where the interstitial velocity at each zone is derived analytically under the assumption that solid particles move continuously and the mass transfer mechanism is controlled by liquid-film resistance and pore diffusion. The analytic equations for the SMB interstitial velocity ($u_I$, $u_{II}$, $u_{III}$ and $u_{IV}$) of each zone are found in terms of column dimension, cycle time, purity and feed ratio [Ma and Wang, 1997; Wu et al., 1999; Xie et al., 2000]:

$$Q_I = \varepsilon_b S u_I = \varepsilon_b S \left[ \frac{L_c(1+\phi K_B)}{\tau} - \frac{\ln([1-1/\mathrm{Pu}_{raf}]/\gamma_{feed})}{L_I} \cdot \left( D_{ax,B} + \frac{\phi K_B^2 \cdot \left(\frac{L_c}{\tau}\right)^2}{k_{I,B}(\varepsilon_p + (1-\varepsilon_p)K_B)} \right) \right] \tag{14a}$$

$$Q_{II} = \varepsilon_b S u_{II} = \varepsilon_b S \left[ \frac{L_c(1+\phi K_A)}{\tau} - \frac{\ln([1-1/\mathrm{Pu}_{ext}]/\gamma_{feed})}{L_{II}} \cdot \left( D_{ax,A} + \frac{\phi K_A^2 \cdot \left(\frac{L_c}{\tau}\right)^2}{k_{II,A}(\varepsilon_p + (1-\varepsilon_p)K_A)} \right) \right] \tag{14b}$$

$$Q_{III} = \varepsilon_b S u_{III} = \varepsilon_b S \left[ \frac{L_c(1+\phi K_B)}{\tau} + \frac{\ln([1-1/\mathrm{Pu}_{raf}]/\gamma_{feed})}{L_{III}} \cdot \left( D_{ax,B} + \frac{\phi K_B^2 \cdot \left(\frac{L_c}{\tau}\right)^2}{k_{III,B}(\varepsilon_p + (1-\varepsilon_p)K_B)} \right) \right] \tag{14c}$$

$$Q_{IV} = \varepsilon_b S u_{IV} = \varepsilon_b S \left[ \frac{L_c(1+\phi K_A)}{\tau} - \frac{\ln([1-1/\mathrm{Pu}_{ext}]/\gamma_{feed})}{L_{IV}} \cdot \left( D_{ax,A} + \frac{\phi K_A^2 \cdot \left(\frac{L_c}{\tau}\right)^2}{k_{IV,A}(\varepsilon_p + (1-\varepsilon_p)K_A)} \right) \right] \tag{14d}$$

where S is the cross-section area of the column, $\varepsilon_p$ is the pore voidage, $\gamma_{feed}$ is defined as the feed concentration ratio of B to A ($\gamma_{feed} = C_{B,feed}/C_{A,feed}$), the column length of each zone is referred to as $L_I - L_{IV}$ and the overall mass transfer coefficient (k) is given at each zone for each component. $K_A$ and $K_B$ are the equilibrium constants (or linear adsorption isotherms) of A and B, respectively. Note that the values based on per-particle volume are different from those of the original definition (see Ma and Wang, 1997) and Eq. (5c) is expressed as follows:

$$n_A^* = K_A \cdot C_A \tag{15a}$$

$$n_B^* = K_B \cdot C_B \tag{15b}$$

The third term of the right hand side in Eq. (14) is neglected in an equilibrium case ($k \rightarrow \infty$).

Eq. (14) means that the two purities ($\mathrm{Pu}_{ext}$ and $\mathrm{Pu}_{raf}$) can be specified by a flowrate and the cycle time ($\tau$) on a given column dimension and configuration for linear nonequilibrium TMB systems. That

is, the following relationship is able to be obtained from Eq. (14b) and (14c):

$$Pu_{ext}=f(\tau, Q_{II}) \quad (16a)$$
$$Pu_{raf}=f(\tau, Q_{III}) \quad (16b)$$

As $Q_{II}$ can $Q_{III}$ independently vary adjusting $Q_{ext}$ and $Q_{feed}$, respectively [see Eq. (1b) and (1c)], even keeping constant the other two flowrates ($Q_{rec}$ and $Q_{des}$) and the cycle time ($\tau$), a minimum set of independent variables for the purity constraints in Eq. (13a) is:

$$Pu_{ext}=f(Q_{ext}) \quad (17a)$$
$$Pu_{raf}=f(Q_{feed}) \quad (17b)$$

A minimum set of variables for the pressure drop constraint is obtained in a straightforward manner [see Eq. (13)]:

$$\Delta p=f(Q_{rec}) \text{ or } f(Q_{des}) \quad (18)$$

The above equation means that the pressure drop constraint can be satisfied by adjusting only one of the two flowrates ($Q_{rec}$ and $Q_{des}$).

The objective function Eq. (3a) is considered as a sum of two individual objectives. The first term of the right hand side in Eq. (3a) is changeable with $Q_{ext}$ and the second term is with $Q_{raf}$ which is derived from Eq. (1):

$$Q_{raf} \equiv Q_{des} - Q_{ext} + Q_{feed} \quad (19)$$

Thus, the second term in Eq. (3a) will be a function of $Q_{des}$ or $Q_{feed}$ as a minimum set of variables independent of the first term. Thus, the objective function Eq. (3a) can vary with two variables at least:

$$Pr=f(Q_{ext}, Q_{des}) \text{ or } f(Q_{ext}, Q_{feed}) \quad (20a)$$

The other productivity function Eq. (3b) is the function of $Q_{feed}$:

$$Pr=f(Q_{feed}) \quad (20b)$$

From Eqs. (17), (18) and (20), Eq. (13a) can be treated with the two possible variable sets,

$$X_1=\{Q_{ext}, Q_{feed}, Q_{rec}\} \text{ or } \{Q_{ext}, Q_{feed}, Q_{des}\} \quad (21)$$

The three variables are the minimum variables necessary, but not sufficient, to solve the optimization problem Eq. (13a). The first combination in Eq. (21), $X_1=\{Q_{ext}, Q_{feed}, Q_{rec}\}$, is selected by reason that the subsequent optimization problem Eq. (13b) is directly related to $Q_{des}$. In fact, the desorbent spent can be reduced by adjusting the cycle time, without a loss in purity [Beste et al., 2000; Klatt et al., 2002]. As a result, the variable space decomposed for Eq. (13) is given as:

$$X_1=\{Q_{ext}, Q_{feed}, Q_{rec}\} \quad (22a)$$
$$X_2=\{\tau, Q_{des}\} \quad (22b)$$

Since the variable analysis is based on linear isotherms and true moving bed (TMB) assumption, it is not clear that this approach is useful for (non)linear SMB systems. However, the decomposed prob-

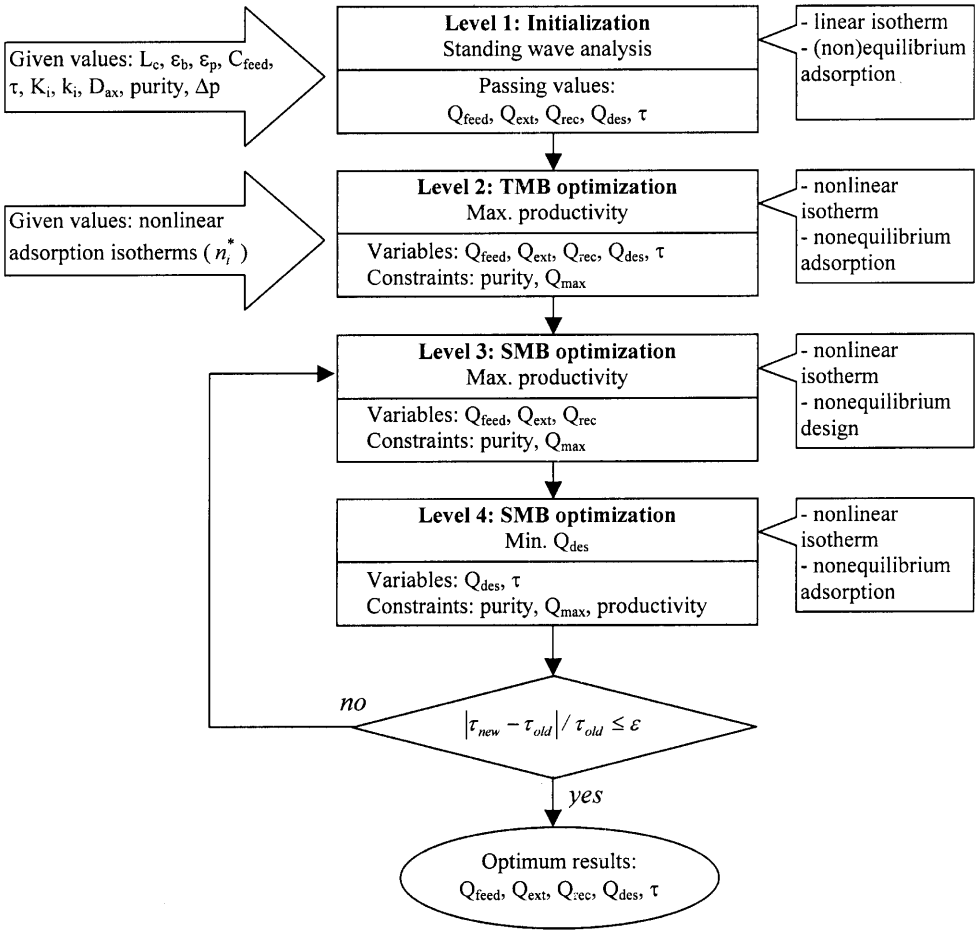


**Fig. 1. MLOP (multi-level optimization procedure) schema for SMB processes.**

lems are in most cases well-conditioned, as will be shown in numerical studies.

The optimization problem using an SQP algorithm will become prohibitive, as the number of iterations increases. To reduce iteration and ensure convergence in the SMB optimization levels, a preconditioning is performed by using the TMB model that is useful to predict the SMB performance [Pais et al., 1998].

## 2. Four Levels from Initialization to Optimization

The preconditioning includes two levels: a rough initialization level and the TMB optimization level for maximum productivity with all the five variables (i.e., cycle time and four flowrates). Notice that the TMB optimization problem is normally easier to solve by using an SQP algorithm than the SMB optimization problem. The preconditioning from the TMB model optimization in the second level is expected to accelerate convergence in the SMB optimizations.

Fig. 1 shows complete four levels including the initialization level, the TMB optimization level and the two SMB optimization levels. The standing wave analysis [Ma and Wang, 1997] derived in the case of linear isotherms [see Eq. (14)] is employed in the initialization level, providing linear equilibrium constants assumed. The initial operating conditions analytically obtained from the first level are shown to be good starting points for the following TMB (true moving bed) optimization level, but the solution quality of the first level becomes worse as nonlinearity of the system considered increases. In the second level, productivity is maximized by adjusting the five operating variables, using the TMB model including nonlinear isotherms, nonequilibrium adsorption kinetics and countercurrent liquid/solid convections.

Additional fine-tuning is required for the operating conditions resulting from the TMB optimization, because purity constraints are not satisfied any longer in the SMB model simulation (i.e., port switching instead of solid movement) that is more realistic than the TMB model simulation [Beste et al., 2000]. Since an optimization based on the SMB model with the five operating variables often fails to converge (or produces local optima unsatisfactory) with the SQP algorithm, the five variables are decomposed into two variable spaces in the next two SMB optimization levels, as mentioned above.

In the third level, productivity is again optimized by adjusting three flowrates within satisfactory purities, starting at the optimum points of the second level. The two remaining variables (desorbent flowrate and cycle time) are used in the fourth level to minimize the desorbent consumption. The two variable spaces are carefully selected on the basis of the analytic equations from the standing wave analysis [Ma and Wang, 1997], as mentioned earlier. Even though iteration between the two SMB optimization levels is basically needed with an iteration tolerance, a satisfactory solution can be obtained without iteration or with a couple of iterations due to the TMB optimization level preceded.

**Level 1**: The first level is to find initial starting points using linear and (non)equilibrium models with a specified column design and purity. The standing wave analysis in Eq. (14) gives an initial value of the four flowrates under the assumption of linear adsorption isotherms. That is, equilibrium constants ($K_i=dn_i^*/dC_i$) are provided roughly even in nonlinear cases. An analytical solution is quickly obtained from Eq. (14), but its quality is limited in the nonlinear cases, as will be shown in Table 3 and 5.

The solid velocity ($v_S$) should be decided between the liquid velocity of a slow-going component (B) and that of a fast-going component (A) for separation [Ma and Wang, 1997] in zone III (i.e., interval between feed-raffinate). Assuming equilibrium adsorption and linear isotherms, the switching time ($\tau$) is analytically obtained:

$$\tau_A<\tau<\tau_B \tag{23}$$

where $\tau_A$ and $\tau_B$ are the time required to path the one column length for A and B components, respectively:

$$\tau_A=\frac{L_c}{u_{III}}(1+\phi K_A) \tag{24a}$$

$$\tau_B=\frac{L_c}{u_{III}}(1+\phi K_B) \tag{24b}$$

Since the interstitial velocity in the zone III ($u_{III}$) is defined as Eq. (1c), all of the four flowrates are required to know $\tau_A$ and $\tau_B$. When the rough range of the four flowrates is known, the rough range of the switching time can be identified. Furthermore, the following condition should be satisfied in Eq. (14):

$$Q_{III}\geq Q_{II} \tag{25}$$

Assuming that $L_{II}=L_{III}=L$, $D_{ax,A}=D_{ax,B}\approx=0$, $Pu_{ext}=Pu_{raf}=Pu$, $\gamma_{feed}=1$ and $k_{II,A}=k_{III,B}=k$ in Eq. (14b) and (14c), the condition Eq. (23) is expressed for the cycle time ($\tau$):

$$\tau\geq\frac{-\ln(1/Pu-1)L_c}{kL}\frac{(K_A^2/(\varepsilon_p+(1-\varepsilon_p)K_A)+K_B^2/(\varepsilon_p+(1-\varepsilon_p)K_B))}{(K_B-K_A)} \tag{26}$$

The above equation implies that there is a minimum cycle time at the given purity constraint and a large cycle time ($\tau$) is obliged in some cases where the mass transfer rate (k) is small, e.g., when large particles are used as adsorbent in preparative chromatography. Since the initialization level plays an important role in solving next TMB optimization level, other techniques (e.g., the triangle theory, Mazzotti et al., 1997) or expert experiences can be taken into account instead of the standing wave analysis.

**Level 2**: The second level is to maximize productivity by using the nonlinear/nonequilibrium TMB model for the four flowrates (desorbent, extract, feed and recycle) and the cycle time. The problem can be formulated under the same constraints as in Eq. (12a):

$$\underset{X}{\text{Max}}\ Pr, X=Q_{des}, Q_{ext}, Q_{feed}, Q_{rec} \text{ and } \tau \tag{27}$$

When Eq. (3a) is used as the productivity objective function, the average concentrations of extract ($\overline{C}_{ext,B}$) and raffinate ($\overline{C}_{raf,A}$) are obtained from the TMB model Eq. (5a), (9), (5c) and (6)-(7) during the cycle time corresponding to the final shifting in the SMB operation.

Even though the SMB operating variables (i.e., flowrates and cycle time) can be optimized by using the TMB approach, the quality of the prediction of the TMB model is limited due to cyclic behaviors in the SMB operation [Strube et al., 1997]. It is therefore necessary to perform optimization based on the SMB model, as mentioned earlier.

**Level 3**: Purity is in general deteriorated in the SMB model solution, compared with the TMB model solution. Thus, purity constraints in Eq. (13a) will not be satisfied at the initial values obtained from the level 2. Using the nonlinear/nonequilibrium SMB model in the third level, productivity is again optimized for only three flowrates (extract, feed and recycle).

$$\underset{X_1}{\text{Max}}\ \text{Pr}, X_1 = Q_{ext}, Q_{feed} \text{ and } Q_{rec} \tag{28}$$

In employing Eq. (3a) for the productivity function, the average concentrations of extract ($\overline{C}_{ext,B}$) and raffinate ($\overline{C}_{raf,A}$) are obtained from the SMB model simulation during one cycle time at the final shifting. The third level focuses on making the purity constraints satisfied in the SMB approach by adjusting the minimum set of the optimization variables (i.e., three flowrates).

**Level 4**: The final level is to minimize desorbent consumption constrained by the maximum productivity obtained from the third level, adjusting desorbent flowrate and the cycle time. The other three operating variables remain constant. Two optimization problems are formulated according to the productivity functions Eq. (3a) and (3b):

$$\begin{aligned}
&\underset{X_2}{\text{Min}}\ Q_{des}, X_2 = Q_{des} \text{ and } \tau \\
&\text{s.t. } \text{Pr}_{ext} \geq \text{Pr}_{ext}^{max} \\
&\text{Pr}_{raf} \geq \text{Pr}_{raf}^{max} \\
&\quad (\text{Pu})_{ext} \geq a_1 \\
&\quad (\text{Pu})_{raf} \geq a_2 \\
&\quad (Q_{rec} + Q_{des}) \leq a_3
\end{aligned} \tag{29a}$$

$$\begin{aligned}
&\underset{X_2}{\text{Min}}\ Q_{des}, X_2 = Q_{des} \text{ and } \tau \\
&\text{s.t. } (\text{Pu})_{ext} \geq a_1 \\
&\quad (\text{Pu})_{raf} \geq a_2 \\
&\quad (Q_{rec} + Q_{des}) \leq a_3
\end{aligned} \tag{29b}$$

In Eq. (29b), the productivity remains constant, because $Q_{feed}$ is fixed [see Eq. (3b)]. The maximum flowrate constraint is automatically satisfied in the two optimization problems, because $Q_{rec}$ is fixed and $Q_{des}$ is minimized. The optimization problem starts at the resulting points in the third level. When $Q_{des}$ decreases under the same $Q_{ext}$, $Q_{feed}$ and $Q_{rec}$, $Q_I$, $Q_{II}$, $Q_{III}$ and $Q_{raf}$ also decrease [see Eq. (1) and (19)]. According to the triangle theory [Mazzotti et al., 1997], zones II and III of the TMB unit play a key role in performing the separation, and separation performance (e.g., purity) can be fixed at a given zone velocity ratio to the solid velocity in the two zones ($u_{II}/v_S$ and $u_{III}/v_S$). To keep the same zone velocity ratio to the solid velocity (i.e., to obtain the same purity or the higher purity) by decreasing $u_{II}$ and $u_{III}$, it is evident that $\tau$ should be increased. As will be shown in the case studies, the desorbent consumption is reduced increasing the cycle time ($\tau$).

If the difference of the cycle times is larger than a certain tolerance, the third and/or fourth levels are repeated. To our experience, the TMB optimization problem in level 2 converges better than the SMB optimization problem. In order to accelerate convergence and to treat two objective functions, the original SMB optimization problem, Eq. (2), is decomposed into the two SMB optimization problems in this MLOP. However, it may be a hard computational task to repeat the decomposed optimization problem with a severe cycle time tolerance ($\varepsilon$). Thus, a large tolerance about the cycle time ($|\tau_{new} - \tau_{old}|/\tau_{old} \leq \varepsilon$) in the MLOP will help to avoid excessive iterations and eventual failure of convergence during the iterations. In our numerical studies to be presented, 10% tolerance ($\varepsilon$=0.1) is applied and only 1-2 iterations are needed.

**Remarks**: i) The present MLOP using the SQP optimizer provides local optima rather than global optima, that is, other local optimum points can be found at other starting points. However, if level 3 and level 4 are successfully repeated, it is assured that desorbent consumption in level 3 is reduced on the same or a higher produc-

**Table 2. Operating conditions and simulation parameters for the sugar SMB process[1]**

| | Zone I | Zone II | Zone III | Zone IV |
|---|---|---|---|---|
| Q (ml/min) | 15.88 | 11.0 | 12.67 | 9.1 |
| $v_L$ (cm/min) | 7.22 | 5.0 | 5.76 | 4.14 |
| $D_{ax}$ (cm$^2$/min) | $0.153v_L$ | $0.153v_L$ | $0.153v_L$ | $0.153v_L$ |
| k (min$^{-1}$) | 0.9 (A), 0.72 (B) | 0.9 (A), 0.72 (B) | 0.9 (A), 0.72 (B) | 0.9 (A), 0.72 (B) |
| Pe | 340 | 340 | 340 | 340 |
| St | 6.5 (A), 5.2 (B) | 9.4 (B), 7.5 (A) | 8.1 (A), 6.5 (B) | 11.3 (A), 9.1 (B) |

| Column information | Length ($L_c$, m) | ID (m) | Bed voidage ($\varepsilon_b$) | Pore voidage ($\varepsilon_p$) | Number of columns |
|---|---|---|---|---|---|
| | 52.07 | 2.6 | 0.41448 | 0.5 | 8 (2-2-2-2) |

| Inlet concentration | Feed concentration (g/*l*) | | Desorbent concentration (g/*l*) | |
|---|---|---|---|---|
| | 322 (A) | 363 (B) | 0 (A) | 0 (B) |

| Adsorption isotherm | Glucose (A) | Fructose (B) |
|---|---|---|
| $K_i$ | $n^*_{Glu} = 0.32 \cdot C_{Glu} + 0.0004570 \cdot C_{Fru} \cdot C_{Glu}$ | $n^*_{Fru} = 0.675 \cdot C_{Fru}$ |
| | $K_A = 0.32$ | $K_B = 0.675$ |

| Simulation parameters | N. shiftings ($N_{shift}$) | CFL number ($\nu$) | Shifting time ($\tau$, min) | N. mesh points ($N_m$) | N. time steps ($N_t$) |
|---|---|---|---|---|---|
| | 44 | 0.6 | 16.39 | 41 | 150 |

| Constraints | $Q_{max}$=30 ml/min | $Pu_A^{min}$=97.0% | $Pu_B^{min}$=97.0% |
|---|---|---|---|

[1]All of the design/operation/model parameters are referred to Beste et al. [2000].

tivity in level 4 (see Tables 3 and 5). That is, the MLOP is constructed on a non-worse solution property advancing level by level. ii) When the column dimension and configuration are changed (i.e., for different design parameters), only level 1 and level 2 are repeated rather than the whole levels, because it is considered that the TMB optimization can give a sufficient resolution for design parameter screening. iii) Since there are three optimization steps in the MLOP, it is desirable to use a computationally-efficient solution method for solving the unsteady-state TMB and SMB models described by time-space partial differential equations. iv) A steady-state TMB model will be useful in the second level to reduce the computational time.

## NUMERICAL EVALUATION OF MLOP

To evaluate the MLOP proposed for nonlinear SMB processes, two test examples are selected: i) quasi-linear isotherm and non-equilibrium adsorption model (sugar SMB, Beste et al., 2000) and ii) nonlinear isotherm and nonequilibrium adsorption model (binaphthol SMB, Pais et al., 1998). Design, operation, model, and simulation parameters for the three SMB processes are shown in Tables 2 and 4, respectively. To solve the unsteady-state TMB and SMB models, the conservation element and solution element (CE/SE) method [Lim et al., 2004; Chang, 2002] is used, which gives an accurate solution with a low computational time for adsorption chromatographic problems [Lim and Jørgensen, 2004; Lim et al., 2004]. The computational time required for one simulation of the unsteady-state TMB or SMB model (about 5.5 roundings where one rounding is equal to the total column number) was about 1 and 2 minutes for the two examples, respectively, on a 1.3 GHz PC. In fact, the CE/SE method has shown for convection dominated PDE (or PDAE) systems outstanding performance on accuracy, computational efficiency as well as solution stability [Lim et al., 2004; Motz et al., 2002].

Note that, in the CE/SE simulation, the CFL number ($\nu = v_L \Delta t/\Delta z$) varies with $0.6 \le \nu \le 0.8$ for the two examples, because the number of mesh points ($N_m$) per column and the number of time steps ($N_t$) during one shifting time ($\tau$) are fixed (see Table 2 and 4) while the liquid interstitial velocity ($v_L$) is different for each zone. In these Tables, the maximum CFL number is indicated. Initially, the bed is filled with an inert solution ($C_{A,0}=C_{B,0}=0$ for all columns) and the resin is intact ($n_{A,0}=n_{B,0}=0$ for all columns).

### 1. Quasi-Linear/Nonequilibrium Sugar SMB

The fructose-glucose mixture in an $Na_2CO_3$-water dilute solution is separated by 8-column ion-exchange SMB chromatography packed with a gel-type strong cation exchange resin (commercial name: Lewatit® MDS 1368, $Ca^{2+}$-form, particle i.d.=350 μm) supplied by the Bayer AG [Beste et al., 2000]. All of the design, operation and model parameters in Table 2 are also referred to Beste et al. [2000]. In this case study, a high concentrated feed composition (i.e., $C_{in,A}$=322 g/*l* and $C_{in,B}$=363 g/*l*) is chosen and a quasi-linear adsorption isotherm equation is used (see Table 4). Here A is Glucose and B is Fructose. Each component adsorbs on the resin, forming a complex of sugar and $Ca^{2+}$ rather than ion-exchanging between sugar and $Ca^{2+}$.

The range of the switching time is identified under the linear/equilibrium adsorption assumption with the aid of given flowrate ranges and Eq. (24):

$$10.0 \text{ min} \le \tau \le 20.0 \text{ min} \tag{30}$$

The simulation time corresponds to 44 shifting time ($t_{total}=44\tau$) for each simulation of the TMB or SMB model. Table 3 contains MLOP optimization results where the results from the SMB model are given

**Table 3. Results of the MLOP for the sugar SMB process**

| | Variables[1] | | | | | Simulation results | | | | | Objective functions [SMB] |
|---|---|---|---|---|---|---|---|---|---|---|---|
| | $Q_{des}$ | $Q_{ext}$ | $Q_{feed}$ | $Q_{rec}$ [SMB] | $\tau$ (min) | $Pu_{Ext}$ (%) [SMB] | $Pu_{Raf}$ (%) [SMB] | $Pr_{Ext}$ [SMB] | $Pr_{Raf}$ [SMB] | $Q_{max}$[2] [SMB] | |
| 1st level | 7.26 | 6.26 | 2.19 | 3.76 [13.18] | 12.16 | 84.0 [84.2] | 98.0 [96.6] | 33.5 [35.6] | 23.1 [24.0] | 11.0 [15.9] | Pr=56.6 [59.6][3] $Q_{des}$=7.26 |
| 2nd level | 13.87 | 10.77 | 1.83 | 3.30 [13.63] | 11.09 | 97.0 [95.9] | 97.0 [92.8] | 27.92 [28.15] | 24.30 [25.23] | 17.2 [27.5] | Pr=52.2 [53.4] $Q_{des}$=13.87 |
| 3rd level | 13.87 | 7.38 | 1.19 | 0.07 [9.89] | 11.09 | 98.9 [97.0] | 98.0 [97.0] | 17.90 [19.28] | 17.63 [16.76] | 13.9 [23.8] | Pr=35.5 [36.0] $Q_{des}$=13.87 |
| 4th level | 9.52 | 7.38 | 1.19 | 2.43 [9.89] | 15.35 | 98.8 [97.7] | 99.5 [97.4] | 17.40 [19.29] | 15.45 [16.76] | 11.95 [19.41] | Pr=2.8 [36.0] $Q_{des}$=9.52 |
| 3rd level repeated | 9.52 | 4.49 | 1.24 | 0.05 [6.82] | 15.35 | 99.6 [97.0] | 96.1 [97.0] | 17.67 [20.06] | 18.39 [17.37] | 9.57 [16.43] | Pr=36.0 [37.4] $Q_{des}$=9.52 |
| Reference case[4] | 6.78 | 4.88 | 1.67 | 2.11 [9.10] | 16.39 | 97.4 [89.8] | 95.6 [96.5] | 25.1 [24.5] | 21.1 [23.0] | 8.9 [15.9] | Pr=46.2 [47.5] $Q_{des}$=6.78 |
| Experiment[5] | 6.78 | 4.88 | 1.67 | [9.10] | 16.39 | [81.6] | [92.9] | [27.0] | [20.2] | [15.9] | Pr=[47.2] $Q_{des}$=6.78 |

[1]All flowrates has the units [ml·min$^{-1}$].

[2]$Q_{max}=Q_{des}+Q_{rec}$.

[3]Productivity has the units [g·hr$^{-1}$·*l*$^{-1}$] based on the total resin volume ($V_S=(1-\varepsilon_b)L_cSN_c$), see Eq. (3a) for definition.

[4]The reference case is referred to Beste et al. [2000].

[5]The experimental data reported by Beste et al. [2000] are obtained at the middle of the cycle time in the 9.5 roundings (76 shiftings).

**Table 4. Operating conditions and simulation parameters for the binaphthol SMB process[1]**

| | Zone I | Zone II | Zone III | Zone IV |
|---|---|---|---|---|
| Q (ml/min) | 56.83 | 38.85 | 42.49 | 35.38 |
| $v_L$ (cm/min) | 26.77 | 18.30 | 20.02 | 16.67 |
| $D_{ax}$ ($cm^2$/min) | $0.00525 \cdot v_L$ | $0.00525 \cdot v_L$ | $0.00525 \cdot v_L$ | $0.00525 \cdot v_L$ |
| k ($min^{-1}$) | 6.0 | 6.0 | 6.0 | 6.0 |
| Pe ($L_c v_L / D_{ax}$) | 2000 | 2000 | 2000 | 2000 |
| St ($L_c k / v_L$) | 2.35 | 3.44 | 3.15 | 3.78 |

| Column information | Length ($L_c$, cm) | ID (cm) | Bed voidage ($\varepsilon_b$) | Number of columns | Particle voidage ($\varepsilon_p$) |
|---|---|---|---|---|---|
| | 10.5 | 2.6 | 0.4 | 8 (2-2-2-2) | 0.5 |

| Inlet concentration | Feed concentration (g/l) | | Desorbent concentration (g/l) | |
|---|---|---|---|---|
| | $C_{A,in}=2.9$[1] | $C_{B,in}=2.9$[2] | $C_{A,in}=0$ | $C_{B,in}=0$ |

| Adsorption isotherm | $n_A^* = \frac{2.69C_A}{1+0.0336C_A+0.0466C_B} + \frac{0.1C_A}{1+C_A+3C_B}$ | $n_B^* = \frac{3.73C_B}{1+0.0336C_A+0.0466C_B} + \frac{0.3C_B}{1+C_A+3C_B}$ |
|---|---|---|
| $K_i$ | $K_A=2.2$ | $K_B=3.1$ |

| Simulation parameters | N. shiftings ($N_{shift}$) | CFL number ($\nu$) | Shifting time ($\tau$, min) | N. mesh points ($N_m$) | N. time steps ($N_t$) |
|---|---|---|---|---|---|
| | 43 | 0.7 | 3.0 | 31 | 300 |

| Constraints | $Q_{max}$=60 ml/min | $Pu_A^{min}$=97.0% | $Pu_B^{min}$=96.0% |
|---|---|---|---|

[1]All of the design/operation/model parameters are referred to Pais et al. [1998].

**Table 5. Results of the MLOP for the binaphthol SMB process**

| | Variables[1] | | | | | Simulation results | | | | | Objective functions [SMB] |
|---|---|---|---|---|---|---|---|---|---|---|---|
| | $Q_{des}$ | $Q_{ext}$ | $Q_{feed}$ | $Q_{rec}$ [SMB] | $\tau$ (min) | $Pu_{Ext}$ (%) [SMB] | $Pu_{Raf}$ (%) [SMB] | $Pr_{Ext}$ [SMB] | $Pr_{Raf}$ [SMB] | $Q_{max}$[2] [SMB] | |
| $1^{st}$ level | 16.38 | 10.46 | 1.90 | 19.38 [26.15] | 3.29 | 64.6 [91.3] | 78.4 [90.2] | 0.75 [1.05] | 0.38 [0.79] | 35.76 [42.53] | Pr=1.13 [1.84][3] $Q_{des}$=16.38 |
| $2^{nd}$ level | 25.91 | 19.62 | 6.76 | 22.04 [29.46] | 3.006 | 96.0 [97.2] | 97.0 [89.4] | 3.83 [3.67] | 4.00 [4.35] | 47.9 [55.3] | Pr=7.83 [8.02] $Q_{des}$=25.9 |
| $3^{rd}$ level | 25.91 | 20.13 | 5.46 | 22.34 [29.76] | 3.006 | 92.0 [96.0] | 99.1 [97.0] | 3.06 [3.33] | 3.09 [3.44] | 48.2 [55.7] | Pr=6.15 [6.77] $Q_{des}$=25.9 |
| $4^{th}$ level | 22.94 | 20.13 | 5.46 | 22.34 [29.76] | 3.252 | 92.4 [96.0] | 99.5 [97.3] | 3.09 [3.33] | 3.09 [3.44] | 45.2 [52.7] | Pr=6.18 [6.77] $Q_{des}$=22.9 |
| Reference case[4] | 21.45 | 17.98 | 3.64 | 27.95 [35.38] | 3.0 | 96.5 [93.7] | 99.2 [96.5] | 1.96 [2.1] | 1.99 [2.14] | 49.4 [56.7] | Pr=3.95 [4.24] $Q_{des}$=21.45 |

[1]All flowrates has the units [$l \cdot min^{-1}$].
[2]$Q_{max}=Q_{des}+Q_{rec}$.
[3]Productivity has the units [$g \cdot hr^{-1} \cdot l^{-1}$] based on the total resin volume ($V_S=(1-\varepsilon_b)L_c S N_c$), see Eq. (3a) for definition.
[4]The reference case is referred to Pais et al. [1998].

in brackets. For the reference case described in Table 2, its simulation results are also shown and its experimental data are referred to Beste et al. [2000] in Table 3. The productivity function Eq. (3a) is employed.

For the reference case by Beste et al. [2000], our simulation results from the SMB models show a little difference from those of Beste et al. [2000], e.g., 2-5% both in purity and productivity (see Table 7 in Beste et al., 2000). Their SMB simulation results are obtained by using the method of lines with an implicit Gear-type time integrator on 64 mesh points, and concentrations for evaluation of purity and productivity are not time-averaged over the cycle time but are measured at the middle of the cycle time. It is worth noting that the productivity and purity are conflicting each other, because the productivity is obtained at the minimum allowable purities (see the $2^{nd}$ and $3^{rd}$ levels in Table 3). Thus, the higher the purity constraints, the lower the productivity.

Since the adsorption isotherm is quasi-linear, the standing wave analysis gives good starting points in the initialization level [see Fig. 2(a)]. Through the TMB optimization constrained by 97% purity both in extract and in raffinate, all of the five variables are adjusted. Fig. 2 compares concentration profiles obtained from the TMB and SMB model in the first and second levels at the middle of the cycle ($t=2/\tau$) of the final shifting ($N_{shift}$=44). Fig. 3 shows the difference of concentration profiles between the two models at three different moments of the cycle time ($t=1$, $2/\tau$ and $\tau$) in the level 2. The purity constraints are not satisfied in the SMB simulation (see

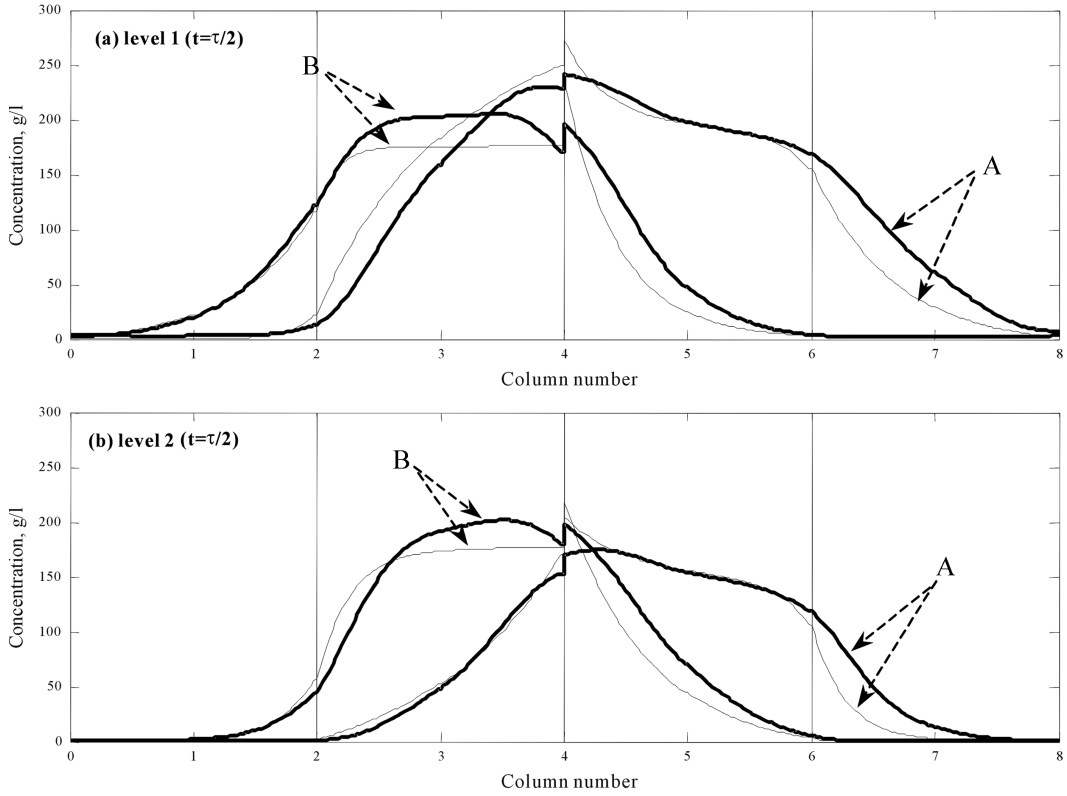


**Fig. 2. Comparison of simulation results between the TMB (thin lines) and SMB (bold lines) models in the level 1 (initialization) and the level 2 (TMB optimization) at the middle of the cycle time (t=τ/2) in the final shifting ($N_{shift}$=44).**

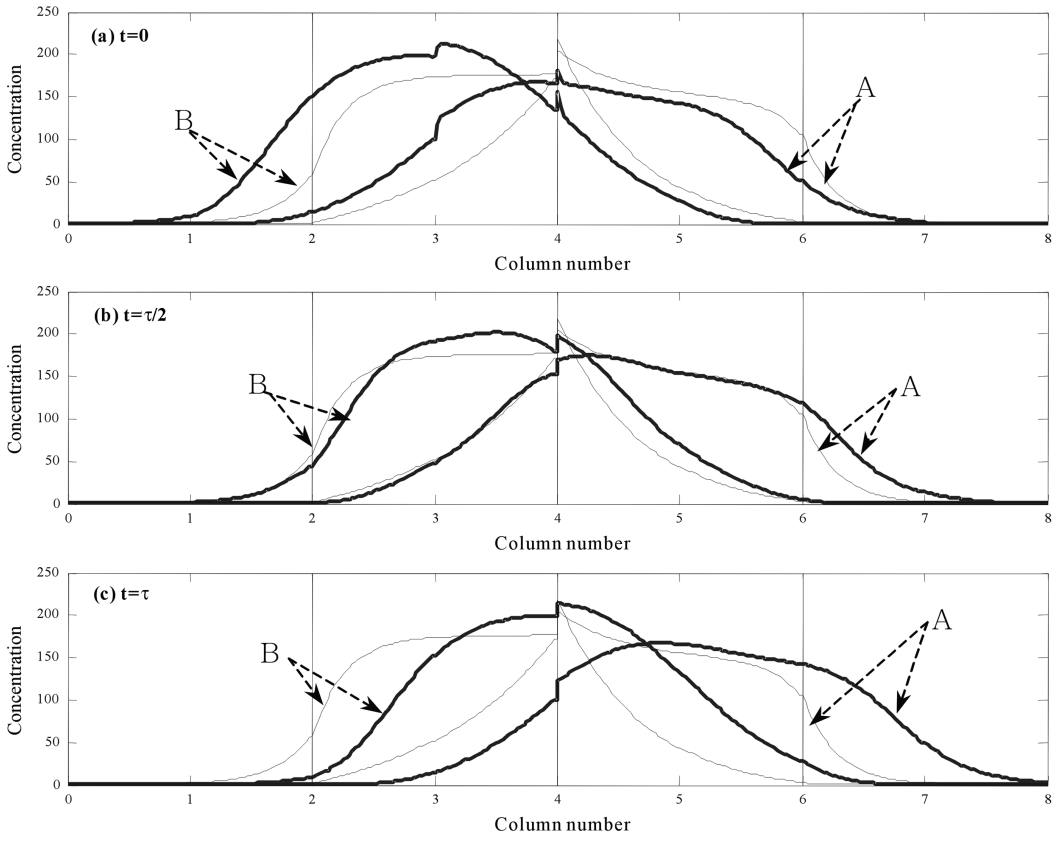


**Fig. 3. Comparison of simulation results between the TMB (thin lines) and SMB (bold lines) models in the level 2 (TMB optimization) at three different moments of the cycle time in the final shifting ($N_{shift}$=44).**

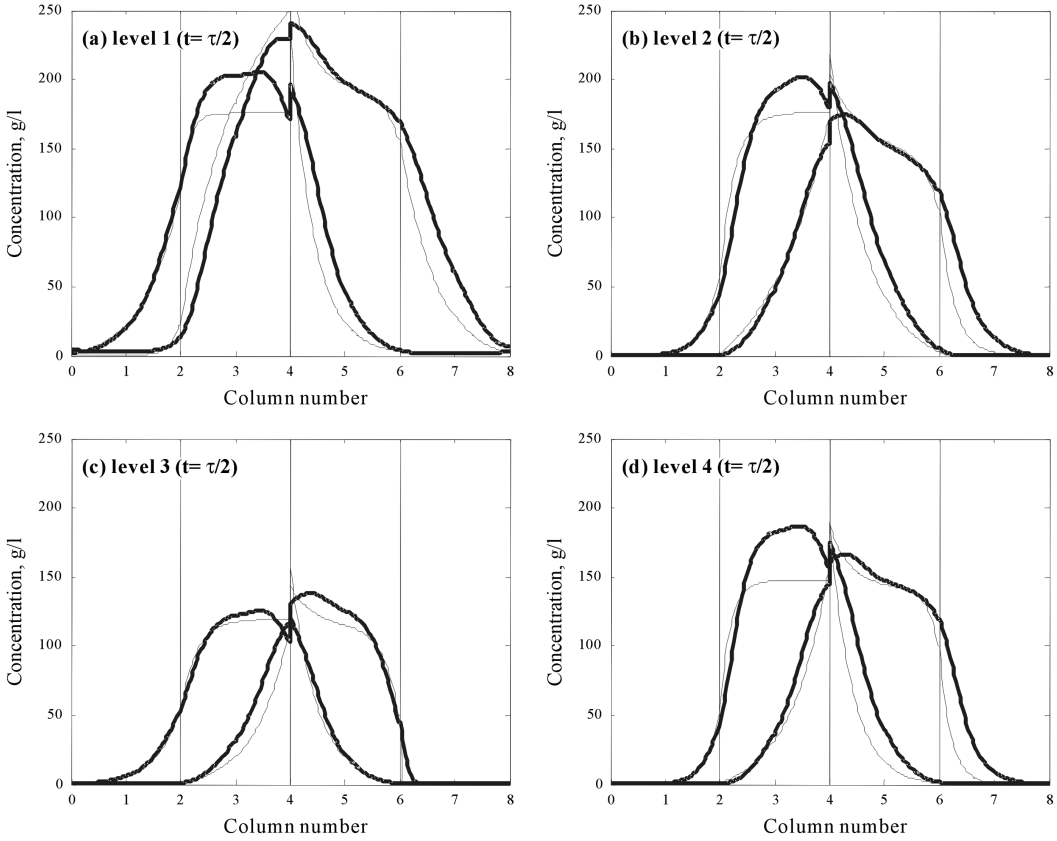


**Fig. 4. Comparison of simulation results between the TMB (thin lines) and SMB (bold lines) models in the levels 1 (initialization), 2 (TMB optimization), 3 and 4 (SMB optimization) at the middle of the cycle in the final shifting ($N_{shift}$=44).**

the 2$^{nd}$ level in Table 3) because of cyclic behavior. It is clear in Fig. 3 that the SMB process can be modeled by the TMB approach, but the cyclic behavior can be predicted only by the SMB approach.

In the third level, the purity constraints are satisfied, reducing the extract, feed and recycle flowrates, but the productivity is much reduced because of a conflicting action between purity and productivity, as mentioned above. In level 4, the desorbent flowrate is decreased up to 31% (13.87→9.52), increasing the cycle time by 38% (11.09→15.35). Purities are slightly increased. Fig. 4 shows concentration profiles along columns obtained from the TMB and SMB models in the four levels such as initialization [Fig. 4(a)], TMB optimization [Fig. 4(b)], SMB optimizations [Fig. 4(c) and (d)]. Here, the profiles are captured at the middle of the cycle in the final shifting ($N_{shift}$=44).

Since the 10% tolerance of the cycle time is exceeded, level 3 is repeated with the following formulation:

$$\begin{aligned} &\underset{X_i}{\text{Max}}\ \text{Pr} \\ &\text{s.t. } (\text{Pu})_{ext} \geq 0.97 \\ &\quad (\text{Pu})_{raf} \geq 0.97 \\ &\quad (Q_{rec} + Q_{des}) \leq 30.0 \\ &\quad (\text{Pr})_{ext} \geq 19.29 \\ &\quad (\text{Pr})_{raf} \geq 16.76 \end{aligned} \tag{31}$$

In the third level repeated, the extract and recycle flowrates are further reduced but the feed and raffinate flowrates increase. Since the productivity is slightly increased by 4% (36.0→37.4), the MLOP is terminated.

Fig. 5 compares the cyclic behavior of the concentrations obtained from the SMB model in level 2, level 3 repeated and in the reference case. Even though the reference case shows the most developed concentration profiles, the purity constrains are not satisfied both in extract and in raffinate. The final solution (dashed lines for level 3 repeated) from the MLOP shows a lower desorbent consumption within satisfactory purities than that obtained from level 2.

Fig. 6 depicts transient time-averaged concentration profiles obtained from the SMB and TMB models in level 3 repeated. The profiles approach toward a quasi-steady state, as the number of shiftings increases. It is found that there is about 10% difference of the absolute value of the concentrations between the TMB and SMB models.

**2. Nonlinear/Nonequilibrium Binaphthol SMB**

The chromatographic resolution of binaphthol enantiomers was considered for simulation purposes in Pais et al. [1998]. The chiral stationary phase used in this process is 3,5-dinitrobenzoyl phenylglycine bonded to silica gel, and a mixture of 72/28 (v/v) heptane/isopropanol is used as desorbent. Since the limit of solubility in this desorbent is 3g/*l* of each enantiomer, the feed composition is determined under a solubility limitation (see Table 4). In Table 4, parameters related to simulation are reported on the basis of the work of Pais et al. [1998]. For adsorption isotherms, a bi-Langmuir type is shown and the equilibrium constants ($K_A$ and $K_B$) are approximated for the initialization level in the MLOP. The range of the switching time is obtained under the linear/equilibrium adsorption assump-

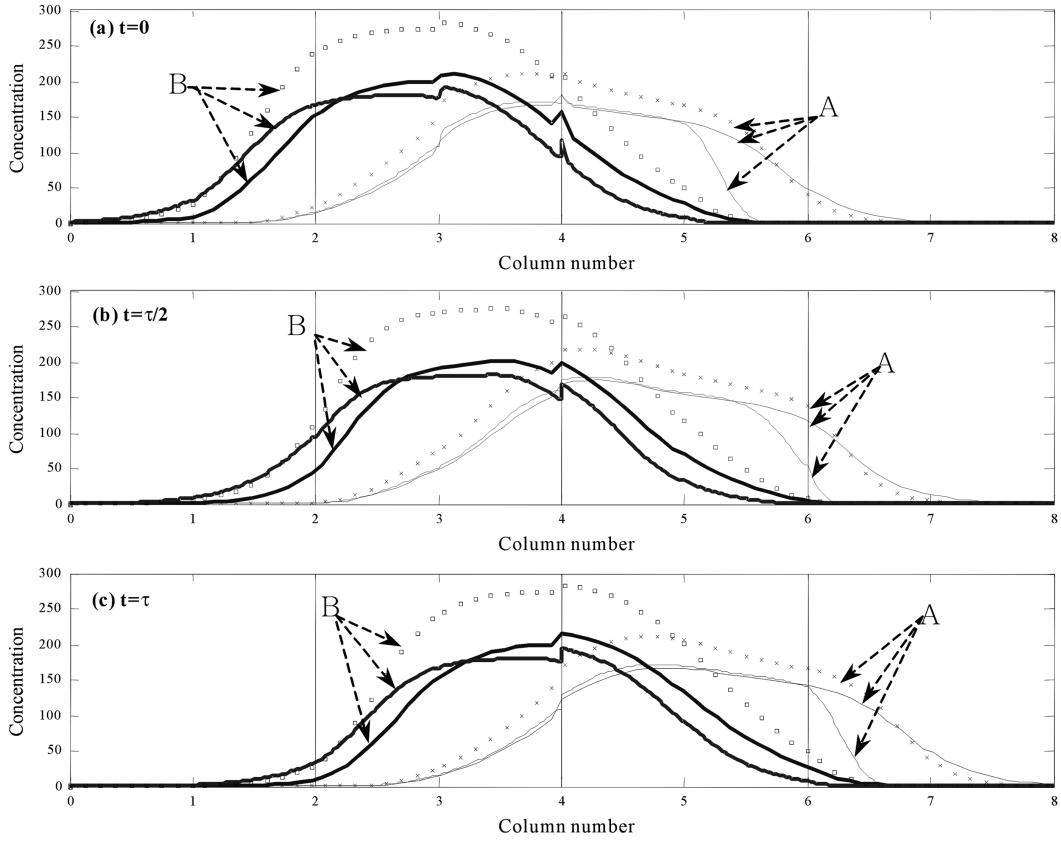


**Fig. 5. Comparison of SMB simulation results for the level 2 (solid lines), level 3 repeated (dashed lines) and the reference case (points) at three different moments of the cycle time ($N_{shift}$=44).**

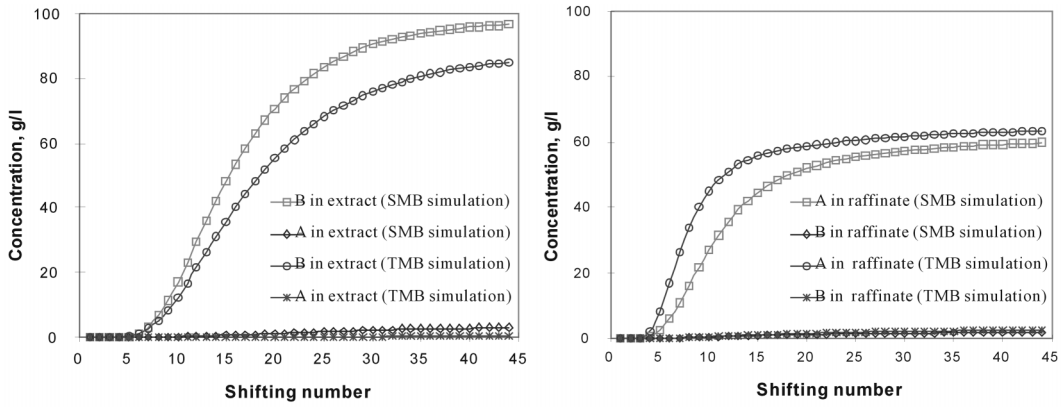


(a) Average concentrations in extract (b) Average concentrations in raffinate

**Fig. 6. Transient of average concentrations obtained from the SMB and TMB models during 44 shiftings (or 5.5 roundings) in level 3 repeated.**

tion with the aide of Eq. (24) and flowrate ranges:

$$1.6 \text{ min} \le \tau \le 4.0 \text{ min} \quad (32)$$

The simulation time corresponds to 43 shifting times ($t_{total}=43\tau$) for each simulation of the TMB or SMB model.

Table 5 summarizes simulation results at each level for the TMB and SMB models, where the results from the SMB model are also given in brackets. The productivity function Eq. (3a) is employed. For the reference case by Pais et al. [1998], our simulation results from the TMB and SMB models have good agreement with those of Pais et al. [1998]. However, slight differences between our and their results are seen, since they used a finite element collocation technique to solve the TMB and SMB models [Pais et al., 2000] on a different number of mesh points. Notice that the productivity and purity are conflicting with each other in this case too, because the productivity is obtained at the minimum allowable purities (see the 3$^{rd}$ level in Table 5).

Initialization points based on the standing wave analysis for the

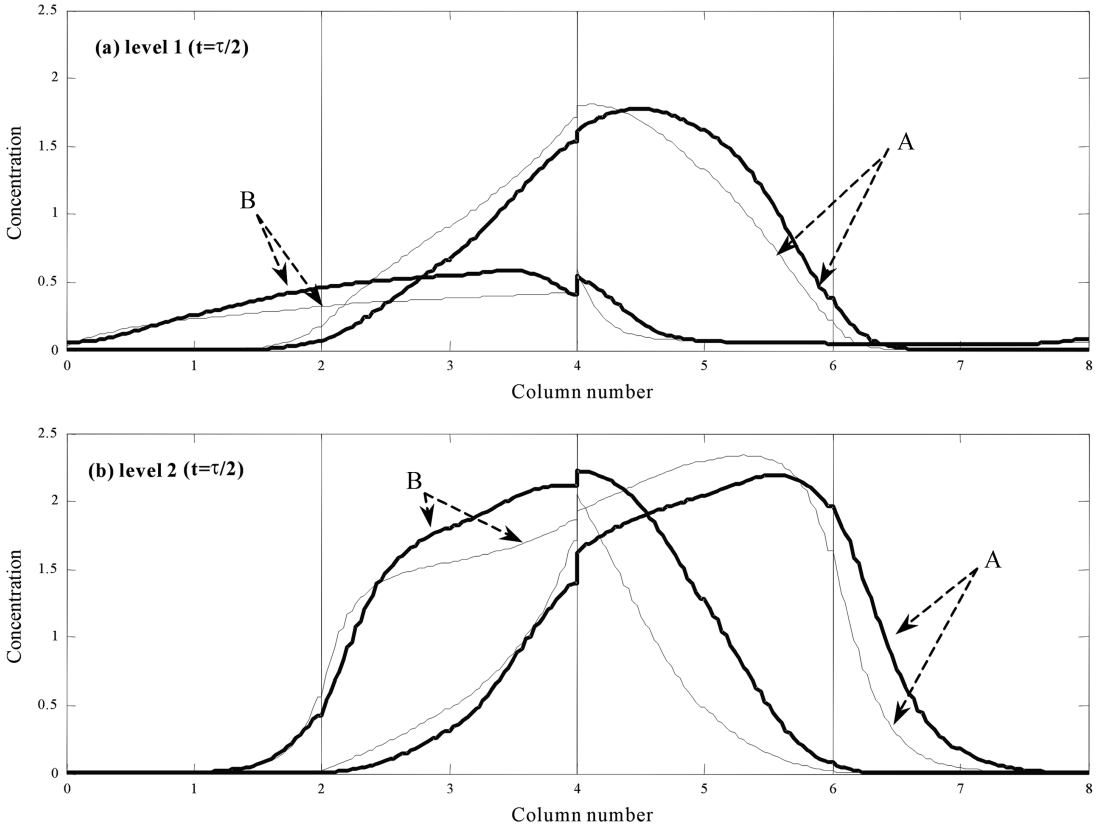


**Fig. 7. Comparison of simulation results between the TMB (thin lines) and SMB (bold lines) models in the level 1 (initialization) and the level 2 (TMB optimization) at the middle of the cycle time (t=τ/2).**

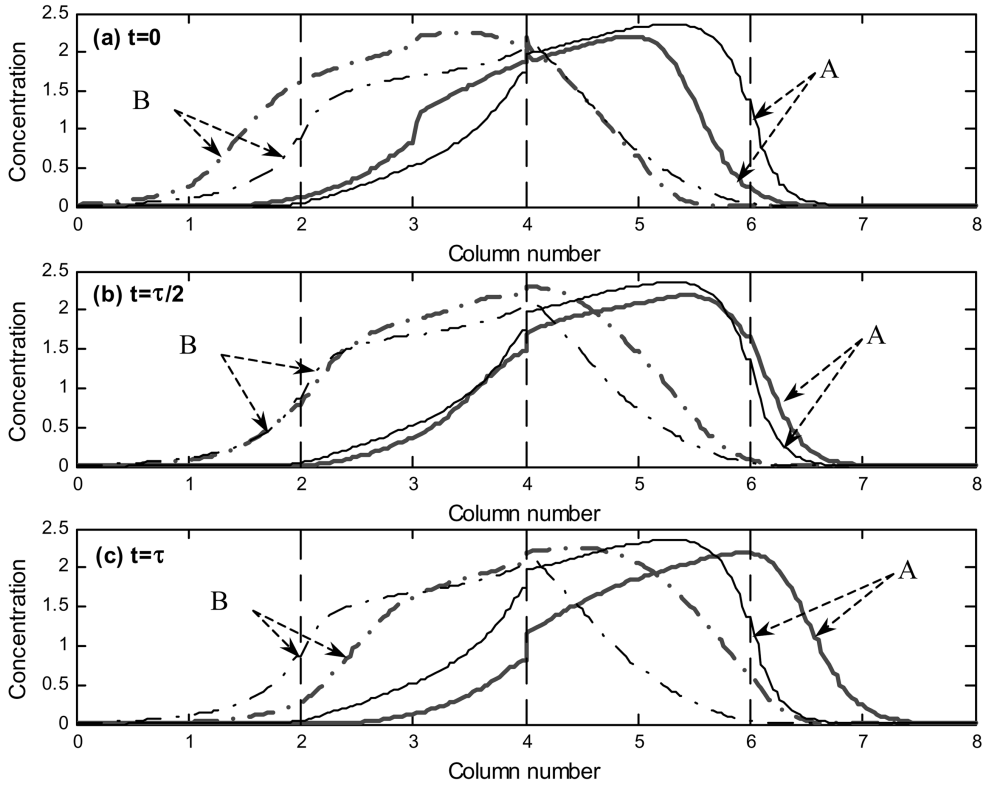


**Fig. 8. Comparison of simulation results between the TMB (thin lines) and SMB (bold lines) models in the level 2 (TMB optimization) at three different moments of the cycle time ($N_{shift}$=43).**

four flowrates give a set of good starting points, but they are somewhat far from optimum points. Since this example is more nonlinear than the previous example, the standing wave analysis based on linear isotherms produces insufficient purities both in extract and in raffinate [see Table 5 and Fig. 7(a)].

The TMB optimization problem Eq. (27) is constrained in this case:

$$0.96 \le Pu_{ext} \quad (33a)$$

$$0.97 \le Pu_{raf} \quad (33b)$$

$$5 \le (Q_{des}+Q_{rec}) \le 60 \quad (33c)$$

For level 1 and level 2, Fig. 7 compares concentration profiles of the TMB and SMB models at the middle of the cycle time after 43 shifting times. It is shown that the TMB model is in good agreement with the SMB model. However, a difference of purity between the two models is not neglectful in the raffinate solution, as reported in Table 5, which comes from the fact that the cyclic behavior in the SMB operation is not taken into account in the TMB model. The purity deviation of the SMB model from the TMB model is much larger than the previous example (i.e., sugar SMB with the quasi-linear adsorption isotherm).

Fig. 8 shows concentration distributions over columns for the two models at the optimum points obtained from the second level (or TMB optimization level). The TMB model (thin lines) produces almost same profiles at the three different time levels (i.e., t=0, $\tau$/2 and $\tau$), as the solid phase moves at the constant velocity. In the SMB model simulation (bold lines), concentration profiles show cyclic behaviors due to the cyclic switching and purity is worse and worse in the raffinate (z=6) as time passes within the cycle time. In fact, the TMB model predicts well only at the middle of the cycle time in the SMB model. To characterize the cyclic behaviors in the SMB operation, the SMB model is useful, as mentioned by Pais et al. [1998].

In the third level, adjusting the three flowrates (extract, feed and recycle), the purity constraints are satisfied and the productivity objective function is maximized. In this SMB model optimization, Eq. (28), purity of the raffinate ($Pu_{raf}$) is improved at the cost of lower productivity, resulting in decrease of the raffinate flowrate (see Table 5).

In level 4, the SMB optimization problem, Eq. (29a), is constrained:

$$3.33 \le Pr_{ext} \quad (34a)$$

$$3.44 \le Pr_{raf} \quad (34b)$$

$$0.96 \le Pu_{ext} \quad (34c)$$

$$0.97 \le Pu_{raf} \quad (34d)$$

$$5 \le (Q_{des}+Q_{rec}) \le 60 \quad (34e)$$

The productivity constraints, Eq. (34a) and (34b), are added into Eq. (33), of which minimum values are obtained from level 3. Satisfying all the constraints, Eq. (34), desorbent consumption is reduced by 11% (25.9→22.9) increasing the cycle time by 8% (3.006→3.252). The desorbent flowrate decreases and the raffinate flowrate thus decreases by the same amount of the desorbent reduction. In order that the productivity [see Eq. (3a)] remains same as that of the level 3 (see Table 5), the purity in raffinate is increased (97.0→97.3), adjusting the cycle time (3.006→3.252). No iteration is per-

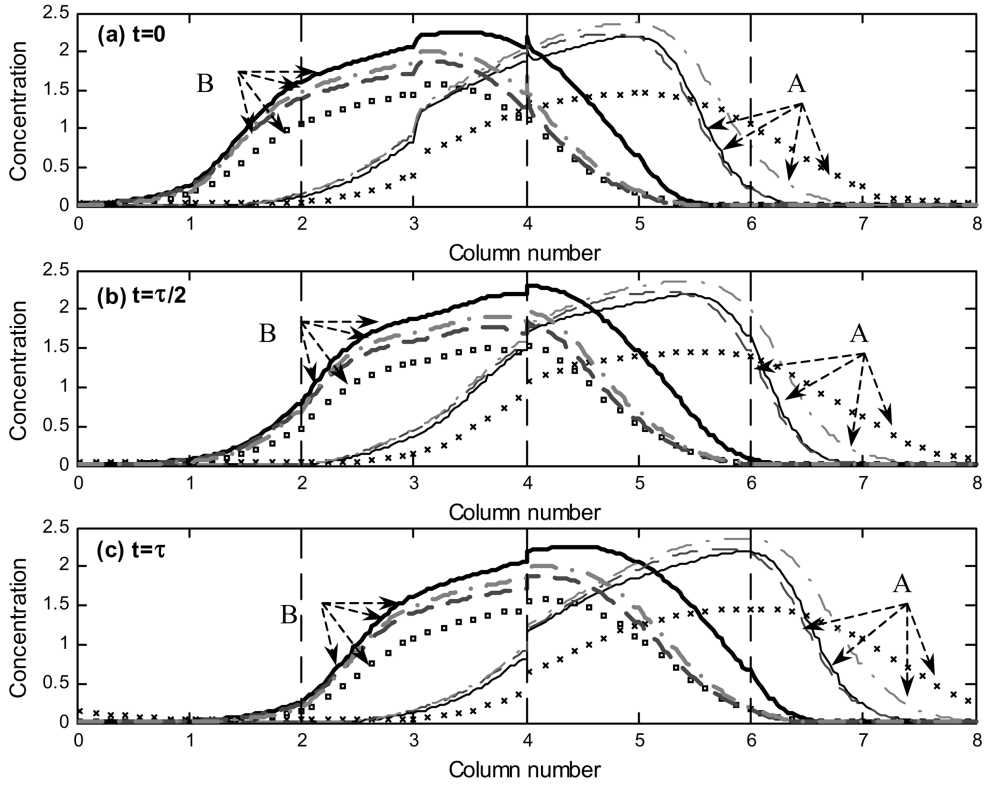


**Fig. 9. Comparison of SMB simulation results for the level 2 (solid lines), level 3 (dashed lines), level 4 (dash-dotted lines) and the reference case (points) at three different moments of the cycle time ($N_{shift}$=43).**

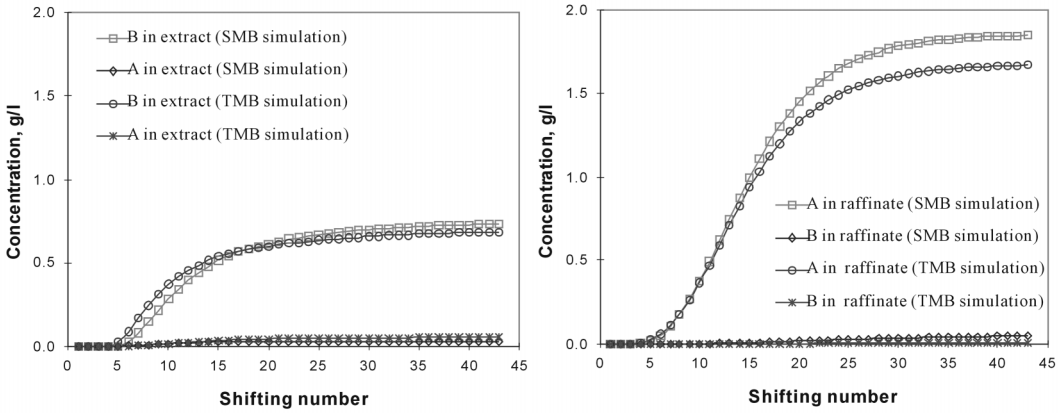


(a) Average concentrations in extract (b) Average concentrations in raffinate

**Fig. 10. Transient of average concentrations obtained from the SMB and TMB models during 43 shiftings in level 4.**

formed between level 3 and 4, as the variation ratio of the cycle time is less than 10%.

In Fig. 9, the reference solution [Pais et al., 1998] with the operating conditions in Table 4 is compared with the MLOP results on the basis of the SMB model simulation. All concentration profiles along the columns from the level 2-4 are developed and controlled better than those of the reference solution. All productivities in the level 2-4 are superior to that of the reference solution, which results from increasing feed, extract and raffinate flowrates. Desorbent consumption in level 4 is not so much increased, i.e., $Q_{des}$=21.45⟶ 22.9, in comparison with the reference solution, due to the increased cycle time.

In Fig. 10, concentration progress in extract and raffinate is shown for simulation results from the SMB and TMB models in level 4. About 10% difference between the TMB and SMB models is seen in the absolute value of the final concentrations.

## CONCLUSION

The multi-level optimization procedure (MLOP) is proposed for model-based optimization to supplement or, in some cases, replace experiments in the nonlinear SMB processes. The MLOP including four levels approaches systematically from initialization to optimization and from simple models (e.g., linear, equilibrium and TMB models) to complex models (e.g., nonlinear, nonequilibrium and SMB models). Through the decomposed optimization, the desorbent consumption is minimized within a satisfactory productivity rather than a compromise between the two objective functions (i.e., productivity and desorbent consumption).

To illustrate potential applications of the procedure, two SMB processes are optimized for higher productivity and lower desorbent consumption in terms of the four flowrates and the cycle time. The SMB operation can be predicted by the TMB model. However, the SMB model is useful to characterize its cyclic behaviors and to simulate more realistically. Similarity and difference between the two models are well shown in these case studies.

For the two cases, this procedure results in improved solutions in terms of productivity and desorbent consumption, compared to reference solutions. It is found from the two case studies that discrepancy between the TMB and SMB models increases, as nonlinearity of the system considered increases.

To reduce the computational load, optimization based on a steady-state TMB model in the second level will be considered in future work.

## ACKNOWLEDGMENT

This research was financially supported by the Danish Energy Authority in the framework of the AMES (Alternative Methods for Energy efficient Separations) project (project #: ENS J. nr. 1273/00-0026). The authors offer their appreciation to Dr. Sin-Chung Chang, who has advised on the application of the space-time CE/SE method to the packed-bed chromatographic model.

## NOMENCLATURE

a : optimization constraint set
A : fast-moving component
B : slow-moving component
CE/SE : conservation element/solution element
$C_{feed}$ : feed composition [g/*l* on liquid volume basis]
$C_i$ : concentration in fluid phase [g/*l* on liquid volume basis]
$\overline{C}_i$ : average liquid concentration over the switching time [g/*l* on liquid volume basis]
$C_{i,0}$ : initial concentration of fluid [g/*l* on liquid volume basis]
$C_{i,in}$ : inlet concentration of fluid at z=0 [g/*l* on liquid volume basis]
$C_{i,out}$ : outlet concentration of fluid at z=$L_c$ [g/*l* on liquid volume basis]
$C_{T,feed}$ : total concentration in feed [g/*l* on liquid volume basis]
$D_{ax}$ : axial dispersion coefficient [$m^2$/min]
k : overall adsorption rate coefficient [1/min]
$K_i$ : equilibrium constant
$L_c$ : column length [m]
LDF : linear driving force
$N_c$ : number of columns
$n_{i,0}$ : initial concentration of solid [g/*l* on particle volume basis]
$n_i$ : concentration in resin or solid phase [g/*l* on particle volume basis]

$n_i^*$ : equilibrium concentration in resin or solid phase [g/*l* on particle volume basis]
$N_m$ : number of mesh points per column
$N_t$ : number of time steps per switching time
$N_{shift}$ : number of shiftings (or switching)
$n_T$ : resin capacity [g/*l* on particle volume basis]
$N_t$ : number of time steps per cycle time
Pe : Peclet number [$=v_L L_c/D_{ax}$]
Pr : total productivity [g/hr/*l*]
$Pr_{ext}$ : productivity in extract [g/hr/*l*]
$Pr_{ext}^{max}$ : maximum productivity in extract [g/hr/*l*]
$Pr_{raf}$ : productivity in raffinate [g/hr/*l*]
$Pr_{raf}^{max}$ : maximum productivity in raffinate [g/hr/*l*]
$Pu_{ext}$ : purity in extract
$Pr_{ext}^{min}$ : allowable minimum purity in extract
$Pu_{raf}$ : purity in raffinate
$Pr_{raf}^{min}$ : allowable minimum purity in raffinate
$Q_I$ : flowrate in the zone I [ml/min]
$Q_{II}$ : flowrate in the zone II [ml/min]
$Q_{III}$ : flowrate in the zone III [ml/min]
$Q_{IV}$ : flowrate in the zone IV [ml/min]
$Q_{des}$ : desorbent flowrate [ml/min]
$Q_{ext}$ : extract flowrate [ml/min]
$Q_{feed}$ : feed flowrate [ml/min]
$Q_{in}$ : inlet flowrate to column [ml/min]
$Q_{max}$ : maximum flowrate of zone I [ml/min]
$Q_{out}$ : outlet flowrate from column [ml/min]
$Q_{raf}$ : raffinate flowrate [ml/min]
$Q_{rec}$ : recycle flowrate [ml/min]
S : cross-section area of column [$cm^2$]
SMB : simulated moving bed
St : Stanton number [$=kL_c/v_L$]
SQP : successive quadratic programming
t : time [min]
TMB : true moving bed
$u_I$ : interstitial fluid velocity in zone I [cm/min]
$u_{II}$ : interstitial fluid velocity in zone II [cm/min]
$u_{III}$ : interstitial fluid velocity in zone III [cm/min]
$u_{IV}$ : interstitial fluid velocity in zone IV [cm/min]
$V_c$ : solid volume of one column [$cm^3$]
$v_L$ : interstitial fluid velocity [cm/min]
$v_S$ : solid velocity [cm/min]
$V_S$ : total solid volume for all columns [$cm^3$]
X : optimization variable set
$X_1$ : optimization variable set for SMB optimization of productivity
$X_2$ : optimization variable set for SMB optimization of desorbent optimization
z : axial direction of column [cm]

**Greek Letters**

$\gamma_{feed}$ : feed concentration ratio of B to A component
$\varepsilon$ : cycle time tolerance
$\varepsilon_b$ : interstitial bed voidage
$\varepsilon_p$ : pore voidage
$\lambda$ : logical variable set for port switching
$\phi$ : phase ratio [$=(1-\varepsilon_b)/\varepsilon_b$]
$\nu$ : CFL number [$=v_L \Delta t/\Delta z$]
$\tau$ : cycle time or shifting time [min]
$\tau_A$ : time for fast-moving component A to reach one column length [min]
$\tau_B$ : time for slow-moving component B to reach one column length [min]
$\xi$ : relaxation factor of productivity
$\Delta p$ : pressure drop in columns [=Pa]
$\Delta t$ : uniform time step size [=min]
$\Delta z$ : uniform spatial step size [=cm]

## REFERENCES


Beste, Y. A., Lisso, M., Wozny, G. and Arlt, W., "Optimization of Simulated Moving Bed Plants with Low Efficient Stationary Phases: Separation of Fructose and Glucose," *J. Chromatogr. A*, **868**, 169 (2000).

Biressi, G., Ludemann-Hombourger, O., Mazzotti, M., Nicoud, R.-M. and Morbidelli, M., "Design and Optimization of a Simulated Moving Bed Unit: Role of Deviations from Equilibrium Theory," *J. Chromatogr. A*, **876**, 3 (2000).

Chang, S. C., "Courant Number Insensitive CE/SE Schemes," 38$^{th}$ AIAA joint propulsion conference, AIAA-2002-3890, Indianapolis, USA (2002).

Juza, M., Mazzotti, M. and Morbidelli, M., "Simulated Moving Bed Chromatography and its Application to Chirotechnology," *Trends in Biotech.*, **18**, 108 (2000).

Kim, Y. D., Lee, J. K. and Cho, Y. S., "The Application of Simulated Moving Bed Chromatography for the Separation Between 2,6- and 2,7-Dimethylnaphthalene," *Korean J. Chem. Eng.*, **18**(6), 971 (2001).

Klatt, K.-U., Dunnebier, G., Hanisch, F. and Engell, S., "Optimal Operation and Control of Simulated Moving Bed Chromatography: A Model-based Approach," *AIChE symposium series 326*, **98**, 239 (2002).

Lee, K. N., "Continuous Separation of Glucose and Fructose at High Concentration Using Two-section Simulated Moving Bed Proesses," *Korean J. Chem. Eng.*, **20**(3), 532 (2003).

Lim, Y. I., Chang, C. S. and Jørgensen, S. B., "A Novel Partial Differential Algebraic Equation (PDAE) Solver: Iterative Conservation Element/solution Element (CE/SE) Method," *Comput. Chem. Eng.*, in press (2004).

Lim, Y. I. and Jørgensen, S. B., "A Fast and Accurate Numerical Method for Solving Simulated Moving Bed (SMB) Chromatographic Separation Problems," *Chem. Eng. Sci.*, in press (2004).

Lim, Y. I., Floquet, P., Joulia, X. and Kim, S. D., "Multiobjective Optimization in Terms of Economics and Potential Environment Impact for Process Design and Analysis in Chemical Process Simulator," *Ind. Eng. Chem. Res.*, **38**(12), 4729 (1999).

Ludemann-Hombourger, O., Pigorini, G., Nicoud, R.-M., Ross, D. S. and Terfloth, G., "Application of the VARICOL Process to the Separation of the Isomers of the SB-553261 Racemate," *J. Chromatogr. A*, **947**, 59 (2002).

Ma, Z. and Wang, N.-H. L., "Standing Wave Analysis of SMB Chromatography: Linear Systems," *AIChE J.*, **40**(10), 2488 (1997).

Mazzotti, M., Storti, G. and Morbidelli, M., "Optimal Operation of Simulated Moving Bed Units for Nonlinear Chromatographic Separations," *J. Chromatogr. A*, **769**, 3 (1997).

Melis, S., Markos, J., Cao, G. and Morbidelli, M., "Separation Between Amino Acids and Inorganic Ions Through Ion Exchange: Development of a Lumped Model," *Ind. Eng. Chem. Res.*, **35**, 3629 (1996).

Motz, S., Mitrovic, A. and Gilles, E.-D., "Comparison of Numerical Methods for the Simulation of Dispersed Phase Systems," *Chem. Eng. Sci.*, **57**, 4329 (2002).

Pais, L. S., Loureiro, J. M. and Rodrigues, A. E., "Chiral Separation by SMB Chromatography," *Sep. Purif. Tech.*, **20**, 67 (2000).

Pais, L. S., Loureiro, J. M. and Rodrigues, A. E., "Modeling Strategies for Enantiomers Separation by SMB Chromatography," *AIChE J.*, **44**(3), 561 (1998).

Powell, M. J. D., "On the Convergence of the vAriable Metric Algorithm," *J. Inst. Math. Appl.*, **7**, 21 (1971).

Proll, T. and Kusters, E., "Optimization Strategy for Simulated Moving Bed Systems," *J. Chromatogr. A*, **800**, 135 (1998).

Strube, J., Altenhoner, U., Meurer, M., Schmidt-Traub, H. and Schulte, M., "Dynamic Simulation of Simulated Moving-bed Chromatographic Processes for the Optimization of Chiral Separations," *J. Chromatogr. A*, **769**, 81 (1997).

Wu, D.-J., Ma, Z. and Wang, N.-H. L., "Optimization of Throughput and Desorbent Consumption in Simulated Moving-bed Chromatography for Paclitaxel Purification," *J. Chromatogr. A*, **855**, 71 (1999).

Xie, Y., Wu, D., Ma, Z. and Wang, N.-H. L., "Extended Standing Wave Design Method for Simulated Moving Bed Chromatography: Linear Systems," *Ind. Eng. Chem. Res.*, **39**, 1993 (2000).

Zhang, Z., Hidajat, K., Ray, A. K. and Morbidelli, M., "Multiobjective Optimization of SMB and Varicol Process for Chiral Separation," *AIChE J.*, **48**(12), 2800 (2002).

Zhang, Z., Mazzotti, M. and Morbidelli, M., "Multiobjective Optimization of Simulated Moving Bed and Varicol Processes using a Genetic Algorithm," *J. Chromatogr. A*, **989**, 95 (2003).